

INFLUENCE OF ULTRASONIC TREATMENT  
ON THE PROPERTIES OF ZnO-MoO<sub>3</sub> OXIDE SYSTEM*Olena Sachuk<sup>1</sup>, Natalya Kopachevska<sup>1</sup>, Lubov Kuznetsova<sup>1</sup>, Valery Zazhigalov<sup>1, \*</sup>,  
Volodymyr Starchevskyy<sup>2</sup>*<https://doi.org/10.23939/chcht11.02.152>

**Abstract.** The effect of ultrasonic treatment (UST) on the physical-chemical properties of zinc-molybdenum system ZnO-MoO<sub>3</sub> (Zn:Mo = 15:85, 25:75, 50:50, 75:25) was studied. Using XRD, FT-IR and DTA methods it was shown that such treatment forms molybdenum suboxides (Magneli phases of Mo<sub>4</sub>O<sub>11</sub> and Mo<sub>8</sub>O<sub>23</sub> composition) and zinc molybdates ( $\alpha$ -ZnMoO<sub>4</sub>, ZnMo<sub>8</sub>O<sub>10</sub>). Specific character of reagents ratio on the formation of these compounds was determined. It was shown that UST changes porous structure of the compositions – non-porous mixture of oxides transforms into composites with micro- and mesopores, resulting in the increase of specific surface and significant reduction of particles size.

**Keywords:** zinc oxide, molybdenum oxide, sonochemistry, molybdenum suboxides, zinc molybdates.

## 1. Introduction

Zinc and molybdenum oxides powders, as well as complex oxide composites on their bases attract attention due to their use as catalysts for luminescent materials [1-3], catalysts and photocatalysts for various processes [4-6], cryogenic phonon-scintillation detectors [7], anticorrosive coatings [1-9], *etc.* Traditional methods of Zn-Mo-O complexes preparing such as hydrothermal method [8, 9], calcination [10], electrochemically activated laser ablation [11], deposition [12], saturation [13], microwave method [14] have a number of significant lacks that are primarily associated with the use of these metals salts, the need to remove anions from these salts, the use of organic solvents or surfactants, process duration and relatively high temperatures of the following thermal

treatment. Use of oxides of these metals as raw materials seems more appealing. However, direct thermal synthesis of oxides leads, as the most of the mentioned methods, to the formation of products with a low specific surface. In [15] the possible use of mechanochemistry for the ZnMoO<sub>4</sub> synthesis from starting oxides for a fairly short period of time was shown. Taking into account that according to [16] mechanochemical processing conditions are somewhat similar to a sonochemical process, this paper studied the changes in the ZnO-MoO<sub>3</sub> system under its ultrasonic processing, as a possible alternative synthesis method.

Effect of ultrasonic treatment is based on the disruption of the liquid medium through the formation of microbubbles filled with gas or vapor liquid (the cavitation phenomenon) in it, leading to the acceleration of chemical reactions and diffusion process, and can significantly reduce the fusion temperature and allows to obtain highly dispersed, homogeneous and chemically pure mixture of solid particles in solutions [17-19].

There are several publications [20-23], which show that the method of ultrasonic treatment can be used for synthesis of, mostly, molybdate double salts using salts (nitrates) of these metals. Data of metal oxides use as initial compounds are absent.

The aim of this work was to study the effect of ultrasonic treatment on physico-chemical properties of zinc oxide-molybdenum system using oxide mixtures with different atomic ratio of the elements Zn:Mo (15:85, 25:75, 50:50, 75:25).

## 2. Experimental

### 2.1. Materials and Synthesis

The samples of zinc-molybdenum system with a molar ratio of ZnO:MoO<sub>3</sub> = 15:85, 25:75, 50:50, 75:25 were prepared by mixing powders of ZnO and MoO<sub>3</sub> (P.A.). Ultrasonic treatment (UST) of compositions (10 g sample) was carried out in an aqueous medium during 1 h

<sup>1</sup> Institute for sorption and problems of endoecology of NAS of Ukraine  
13, General Naumov St., 03164 Kyiv, Ukraine;

<sup>2</sup> Lviv Polytechnic National University  
12, S.Bandery St., 79013 Lviv, Ukraine

\* [zazhigal@ispe.kiev.ua](mailto:zazhigal@ispe.kiev.ua)

© Sachuk O., Kopachevska N., Kuznetsova L., Zazhigalov V.,  
Starchevskyy V., 2017

in UZDN dispersant, which operates under regime of acoustic cavitation at the frequency of 22 kHz and the load of 3 W/cm<sup>2</sup>. The temperature of the reaction medium was maintained at 353 K by circulating cold water around the reactor. After sonication the resulting suspension was dried at 383 K in the air.

## 2.2. Analysis Methods

X-ray analysis of samples was carried out at PW 1830 diffractometer (Philips) with the usage of CuK $\alpha$ -rays. Crystallite size ( $L$ ) for the most intense reflections was calculated by Scherrer equation:

$$L = \frac{KI}{b \cos \Theta} \quad (1)$$

where  $K$  – constant depending on the crystals form ( $K = 0.9$ );  $\lambda$  – length of X-ray wave (for CuK $\alpha$   $\lambda \approx 0.154$  nm);  $\beta$  – peak width at half height, radians;  $\Theta$  – diffraction angle.

FT-IR spectra were recorded at room temperature in the air by "Spectrum-One" spectrometer (Perkin-Elmer Instruments) in the range of 4500–400 cm<sup>-1</sup> in the transmission mode (sample/KBr = 1:20 w/w).

Thermogravimetric analysis was carried out on DERIVATOGRAPH-Q F.Paulik, J.Paulik, L.Erdey (MOM, Hungary) system in the air within the temperature range of 293–1073 K at a heating rate of 10°/min, sensitivity of 100 mg and sample weight of 200 mg.

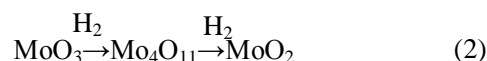
Isotherms of nitrogen adsorption-desorption at 77 K were obtained using NOVA-2200 Gas Sorption Analyzer (Quantachrome, USA). According to BET and BJH methods the specific surface area and distribution of pore volume by samples size were calculated.

## 3. Results and Discussion

On diffractograms of initial oxides mixtures, regardless of the Zn/Mo atomic ratio, we observed ZnO and  $\alpha$ -MoO<sub>3</sub> reflexes of orthorhombic modification with maximum intensity reflection from the lateral plane (040) of molybdenum oxide phase, characterized by lattice parameters  $a = 3.963$  Å,  $b = 13.855$  Å,  $c = 3.699$  Å [24] (Fig. 1). It was found that 1 h ultrasonic treatment for each of the compositions is accompanied by the following general changes in X-ray: firstly, there is a major reduction in the intensity of reflexes with a simultaneous increase of their width, which may indicate the reduction of particle size of initial oxides; secondly, the emergence of new fixed reflexes that characterize the formation of molybdate and molybdenum suboxides of various modifications (the so-called Magneli phases – Mo<sub>4</sub>O<sub>11</sub>, Mo<sub>8</sub>O<sub>23</sub> [25], in which the average degree of oxidation of molybdenum is +5.5 and +5.75, respectively). At the same

time, each of the compositions has some individual features.

In case of ultrasonic activation of ZnO/MoO<sub>3</sub> = 15:85 composition the relative intensity of reflex (040) of molybdenum oxide significantly reduces, and the intensity of the reflection from the plane (021) of the same orthorhombic modification  $\alpha$ -MoO<sub>3</sub> [26] reaches maximum (Fig.1, curve 2). At the same time, after the ultrasonic treatment of the sample its diffractogram fixes new reflexes that show the formation of a stable phase  $\gamma$ -Mo<sub>4</sub>O<sub>11</sub> orthorhombic modification. The formation of this phase as an intermediate product of MoO<sub>3</sub> to MoO<sub>2</sub> reducing may be caused by the presence of hydrogen molecules [25], formed by ultrasonic treatment in the aqueous solution [20]. Estimation of quantity of these oxides in the sample shows that  $\alpha$ -MoO<sub>3</sub> content is 86.1 %, and  $\gamma$ -Mo<sub>4</sub>O<sub>11</sub> phase – 13.9%.



Diffractogram of Zn/Mo = 25:75 sample (Fig. 1, curve 3) shows that ultrasonic treatment leads to a phase transition of orthorhombic  $\alpha$ -MoO<sub>3</sub> modification in monoclinic  $\beta$ -MoO<sub>3</sub>, the formation of which may be caused by anisotropic destruction of a crystal. At the same time new reflexes are observed on diffractogram that show the formation of two zinc molybdate (as a result of interaction between ZnO and MoO<sub>3</sub>):  $\alpha$ -ZnMoO<sub>4</sub> of triclinic modifications with the domination of reflex from the plane (-220) and lattice parameters  $a = 9.625$  Å,  $b = 6.965$  Å,  $c = 8.373$  Å and ZnMo<sub>8</sub>O<sub>10</sub> of tetragonal modification, which describes the presence of reflections at  $2\theta = 18.52, 19.3, 61.2, 62.0$  and  $66.5^\circ$ .

After ultrasonic treatment of the sample with the equimolar content of zinc and molybdenum oxides its diffractogram (Fig. 1, curve 4) shows reflexes of initial compound  $\alpha$ -MoO<sub>3</sub> and a new phase –  $\beta$ -Mo<sub>8</sub>O<sub>23</sub> of monoclinic modification with the domination of this phase reflection from the plane (-204) and lattice parameters  $a = 16.800$  Å,  $b = 4.040$  Å,  $c = 13.400$  Å. The formation of this metastable compound can be explained by a crystallographic shift in MoO<sub>3</sub>, which is the result of intensive action of the ultrasound, accompanied by ordering in the crystal structure and the removal of oxygen atoms from the surface, resulting in the formation of oxygen vacancies [27]. Lack of zinc oxide reflexes can indicate its amorphization or the formation of X-ray amorphous zinc molybdates.

As a result of the sample processing with an excess of zinc oxide Zn/Mo = 75: 25 on its diffractogram (Fig. 1, curve 5) we can observe reflexes of initial ZnO,  $\beta$ -MoO<sub>3</sub> at  $2\theta = 31.8, 56.0, 65.9$  and  $67.7^\circ$ , and  $\eta$ -Mo<sub>4</sub>O<sub>11</sub> of monoclinic modification, the reflex of this phase from the

plane (810) is the most intensive. Evaluation of the content of these compounds in the sample indicates that the number is 36.0, 34.5 and 29.5 %, respectively.

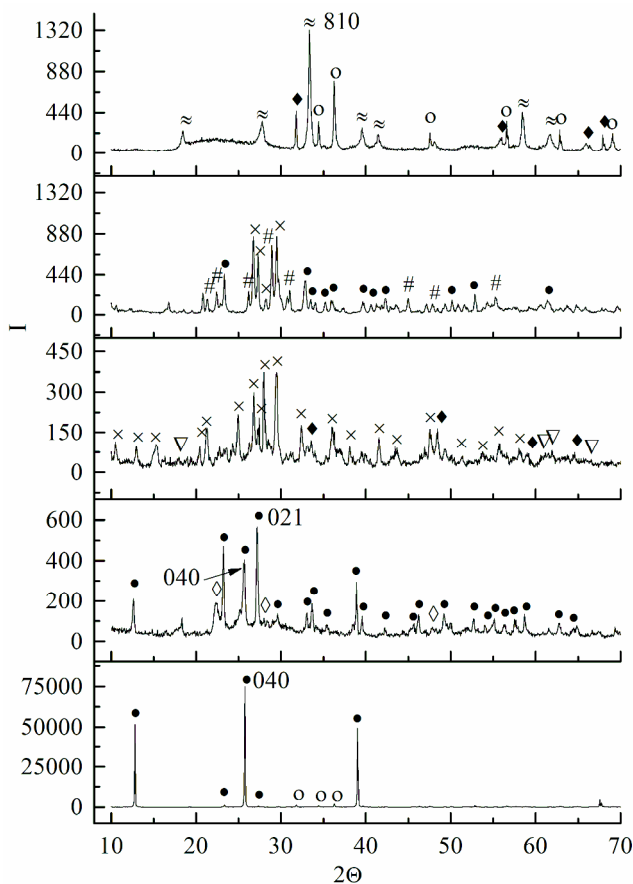


**Fig. 1.** ZnO/MoO<sub>3</sub> diffractograms: initial composition 50:50 (1); after 1 h UST of the compositions 15:85 (2); 25:75 (3); 50:50 (4) and 75:25 (5)  
 ●  $\alpha$ -MoO<sub>3</sub>, ◇  $\gamma$ -Mo<sub>4</sub>O<sub>11</sub>, ×  $\alpha$ -ZnMoO<sub>4</sub>, ◆  $\beta$ -MoO<sub>3</sub>,  
 ▽ ZnMo<sub>8</sub>O<sub>10</sub>, #  $\beta$ -Mo<sub>8</sub>O<sub>23</sub>, ≈  $\eta$ -Mo<sub>4</sub>O<sub>11</sub>, ○ ZnO

Results of X-ray diffraction analysis of samples after ultrasonic treatment are presented in Table 1. The

same table shows the results of particle size calculations carried out using Scherrer equation showing that the process of ultrasonic treatment leads to 2-3 time reduction in the size of crystallites (*L*).

FT-IR results show that ultrasonic treatment increases the intensity of the absorption bands of both stretching vibration of water molecules adsorbed at 3540–3590 cm<sup>-1</sup> and deformation vibrations at 1627 cm<sup>-1</sup> obviously caused by processing conditions. In the spectrum of initial samples (Fig. 2, curve 1 presents the data for the sample ZnO/MoO<sub>3</sub> = 50:50), regardless of the atomic ratio Zn/Mo, the bands of stretching vibrations of asymmetric terminal Mo=O bond at 988 cm<sup>-1</sup>, linear bridging Mo–Mo–O bond at 860 cm<sup>-1</sup> [28, 29] and Zn–O bond at 500 cm<sup>-1</sup> are observed [30, 31]. Due to the samples ultrasonic processing there are some shifts of the absorption bands and the appearance of new bonds vibrations. So in the infrared spectrum of Zn/Mo = 15:85 sample (Fig. 2, curve 2) a sharp reduction in the intensity of the absorption band of Mo=O bond and its shift to 950 cm<sup>-1</sup> is observed. The shift of Mo–O–Mo vibrations toward the high-frequency region (897 cm<sup>-1</sup>) may indicate the increase in bridging bond length. Also the absorption band at 577 cm<sup>-1</sup> appears in the spectrum of this composition, which belongs to the vibrations of linear bridging Mo–O–Mo bond in  $\gamma$ -Mo<sub>4</sub>O<sub>11</sub>.

FT-IR spectrum of Zn/Mo = 25:75 sample (Fig. 2, curve 3) is characterized by absorption bands at 500 and 531 cm<sup>-1</sup> which belong to vibrations of Zn–O bond in oxide and zinc molybdate, respectively. Stretching vibrations at 924 and 897 cm<sup>-1</sup> belong to terminal Mo=O bond (its further shift may be noticed) and linear bridging Mo–O–Mo bonds. At 655 cm<sup>-1</sup> we can observe absorption band which can be attributed to bridging O–Mo–O bond in zinc molybdate. It should be noted that this absorption band is also observed in the infrared spectrum of the sample with equimolar containing of oxides (Fig. 2, curve 4).

Table 1

**XRD results for ZnO/MoO<sub>3</sub> compositions with different component ratio after UST**

Parameter	Zn/Mo atomic ratio				
	Initial (50:50)	15:85	25:75	50:50	75:25
Phase composition	$\alpha$ -MoO <sub>3</sub> , ZnO	$\alpha$ -MoO <sub>3</sub> , $\gamma$ -Mo <sub>4</sub> O <sub>11</sub>	$\alpha$ -ZnMoO <sub>4</sub> , $\beta$ -MoO <sub>3</sub> , ZnMo <sub>8</sub> O <sub>10</sub>	$\beta$ -Mo <sub>8</sub> O <sub>23</sub> , $\alpha$ -MoO <sub>3</sub>	$\eta$ -Mo <sub>4</sub> O <sub>11</sub> , $\beta$ -MoO <sub>3</sub> , ZnO
<i>d</i> *, nm	0.35	0.33	0.30	0.33	0.27
<i>L</i> , nm	81	38	23	33	28

Note: \**d* – position of the reflex with maximal intensity

Simultaneously for ZnO/MoO<sub>3</sub> = 50:50 (Fig. 2, curve 4) we can observe the presence of absorption bands at 832 and 746 cm<sup>-1</sup>, which correspond to a linear bridging Mo–O–Mo bond and angular bridging  $\begin{smallmatrix} & \text{O} \\ & / \backslash \\ \text{Mo} & & \text{Mo} \end{smallmatrix}$  bond in Mo<sub>8</sub>O<sub>23</sub>, respectively [32]. In addition, spectrum of this sample is characterized by a linear absorption band of bridging Mo–Mo–O bond at 882 cm<sup>-1</sup> and Mo=O bond at 924 cm<sup>-1</sup>, confirming the results of XRD about the existence of  $\alpha$ -MoO<sub>3</sub> phase.

In the IR spectrum of the sample with zinc oxide excess (ZnO/MoO<sub>3</sub> = 75:25) we can observe the presence of absorption bands of Zn–O bond at 445 cm<sup>-1</sup>, bridging angular  $\begin{smallmatrix} & \text{O} \\ & / \backslash \\ \text{Mo} & & \text{Mo} \end{smallmatrix}$  bond at 691 and 792 cm<sup>-1</sup> in  $\eta$ -Mo<sub>4</sub>O<sub>11</sub>, linear bridging Mo–O–Mo bond with a strong intensity at 864 cm<sup>-1</sup> and terminal Mo=O at 922 cm<sup>-1</sup>.

Thus, the IR results confirm the structural changes, recorded by XRD, that occur during sonochemical processing of initial oxides mixture.

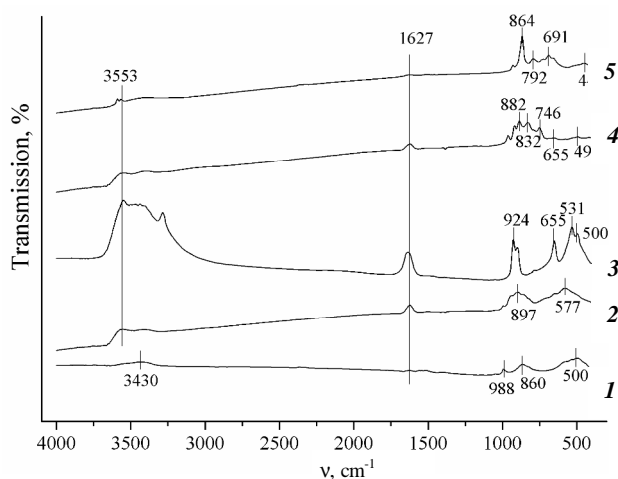


**Fig. 2.** ZnO/MoO<sub>3</sub> IR-spectra: initial composition 50:50 (1); after 1 h UST of the compositions 15:85 (2); 25:75 (3); 50:50 (4) and 75:25 (5)

Thermogram of the initial mixture regardless of oxides atomic ratio (Fig. 3a) shows the presence of endothermal effect on the DTA curve within 413–481 K, which corresponds to the removing of adsorbed water with a small weight loss ( $\approx 6\%$ ). This fact may be due to the small surface area of initial oxides, and absence of micro- and mesopores in it, as it was shown in [15].

The nature of thermoanalytical curves changes after ultrasonic treatment of the samples (Fig. 3b–d). So for the composition Zn/Mo = 25:75 there are two endothermal effects (Fig. 3b) within 348–573 K (peaks at 423 and 498 K), which belong to the removal of adsorbed

water with a total weight loss ( $\approx 42\%$ ). The second endothermal effect – within 963–1043 K with a maximum at 993 K (without weight loss) is associated with melting of nanodispersed MoO<sub>3</sub> (for massive molybdenum oxide  $T_m = 1063$ –1074 K and it is known that the temperature is reduced with increasing the dispersion degree of oxide). A small exothermal effect at 678 K without the weight loss may be associated with the crystallization of zinc molybdates, phases that are formed as a result of processing and can partly be in an amorphous state.

For the composition Zn/Mo = 50:50 (Fig. 3c) we can also observe two endothermal effects associated with the removal of water, with maxima at 448 and 550 K. But first, a fixed weight loss is much lower (16 %) and, secondly, endothermic effect at 550 K is much larger and is shifted to the area of higher temperatures. This fact may indicate the presence of pores in the sample from which desorption of water goes harder. Two weak exothermal effects are observed at 723 and 798 K. The first one may be associated with the crystallization of amorphous zinc molybdate, the formation of which was proposed basing on infrared spectroscopy. The second one, with a slight increase in weight (less than 1 %) can be attributed to the partial oxidation of  $\beta$ -Mo<sub>8</sub>O<sub>23</sub>. Endothermic effect at 1013 K is associated with the melting of nanodispersed MoO<sub>3</sub>.

According to the thermogram of ZnO/MoO<sub>3</sub> = 75:25 sample the removal of water from it is considerably more difficult and consists of three stages. The first stage – with 2% loss of water at the temperature of endothermal effect 448 K and the second – at the temperature of 550 K (3% weight loss) are similar to the previous sample and indicate the presence of a porous structure. The most interesting is the appearance of the third stage with the endothermic effect at 653 K and 8 % weight loss. This may indicate the formation, in this sample as a result of sonochemical processing, of narrow pores, from which water desorption begins at higher temperatures. The exothermal effect at 733 K, which is accompanied by the increase in mass, can correspond to the partial oxidation of  $\eta$ -Mo<sub>4</sub>O<sub>11</sub> and effect at 793 K, without weight changing, corresponds to  $\beta$ -MoO<sub>3</sub>  $\rightarrow$   $\alpha$ -MoO<sub>3</sub> transition (or crystallization of partially amorphous zinc oxide).

Adsorption studies showed that all original compositions are powders with low specific surface (Table 2), and received for them nitrogen sorption isotherms are typical for the mono-poly layer adsorption by micro- or macroporous adsorbents (type II classification IUPAC) without capillary-condensation hysteresis (Fig. 4, curve 1). This means that adsorption in this area occurs not in the pores, but in voids between loosely packed particles of powders. Also distribution curves by pore size shows that the main pore volume of the initial compositions Zn/Mo = 15:85, 25:75, 50:50, 75:25 belongs to macropores with maximum values at 101, 87, 86, 132 nm, respectively.

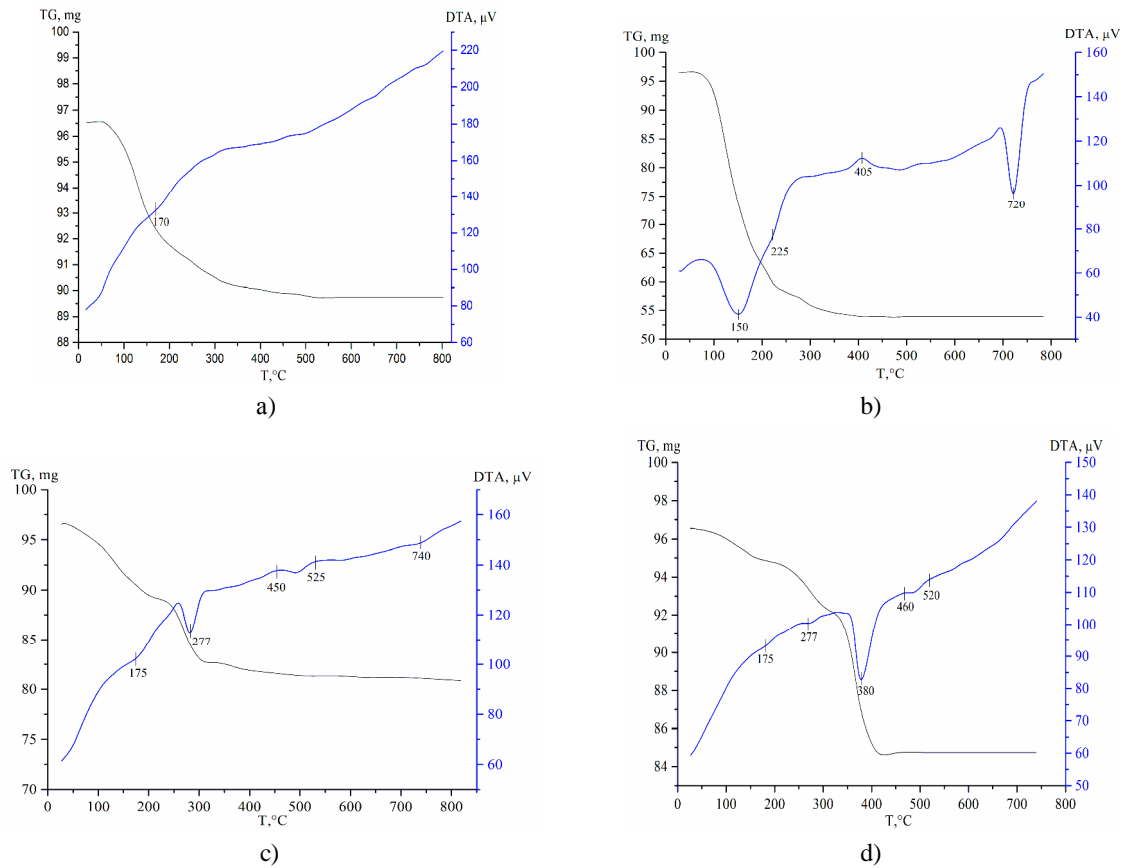


Fig. 3. Thermograms of the initial sample 50:50 (a) and after 1 h UST of the compositions 25:75 (b); 50:50 (c) and 75:25 (d)

Table 2

Characteristics of the samples porous structure before and after UST

Treatment conditions	Composition							
	15:85		25:75		50:50		75:25	
	$S_{BET}, m^2/g$	$V_s, cm^3/g$	$S_{BET}, m^2/g$	$V_s, cm^3/g$	$S_{BET}, m^2/g$	$V_s, cm^3/g$	$S_{BET}, m^2/g$	$V_s, cm^3/g$
Initial	1	0.011	1	0.013	2	0.026	3	0.068
1 h UST	3	0.029	6	0.044	3	0.056	14	0.164

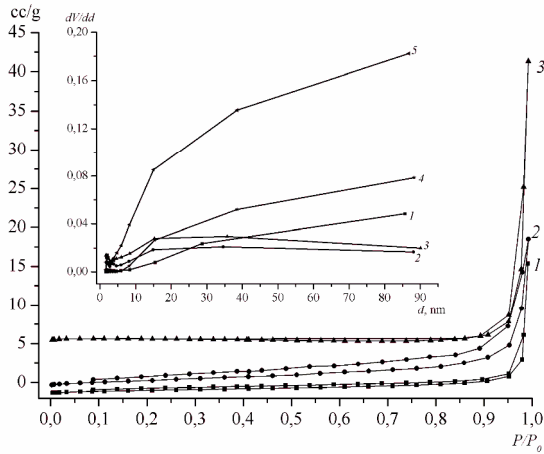


Fig. 4. Isoterms of nitrogen sorption of the initial sample 50:50 (1) and after 1 h UST of the compositions 15:85 (2); 50:50 (3) Insertion: distribution curves by pore size of initial composition 50:50 (1); after 1 h UST of the compositions 15:85 (2); 25:75 (3); 50:50 (4) and 75:25 (5)

Ultrasonic processing of the samples increases the specific surface area and pore volume by 3–6 times (without changing of isotherms type) (Table 2). This is due to the fact that UST of the compounds with low specific surface leads to their dispersion. Also at the distribution curves by pore size for the compositions ZnMo = 15: 85 and 25:75 main pore volume belongs to mesopores that have a maximum value of diameter at 15 nm (Fig. 4, curves 2 and 3), which is in agreement with DTA data. For the samples Zn/Mo = 50:50 and 75:25 the main pore volume belongs to macropores with a diameter of 88 and 87 nm, respectively, the number of mesopores is sharply increased (Fig. 4, curves 4 and 5). It should be noted that for the last compositions the presence of one more maximum is typical (in the area of 1.9 nm), which may be explained by water high-temperature desorption (Fig. 3g).

Comparison of data on ultrasonic and mechanochemical [15] processing of Zn/Mo = 50:50 samples indicates that they are similar, as it was suggested in [16]. Thus, in both cases, the treatment results in partial recovery of molybdenum oxide with the formation of Mo<sub>8</sub>O<sub>23</sub> phase.

## 4. Conclusions

Research shows that ultrasonic treatment of system ZnO/MoO<sub>3</sub> compositions leads to considerable changes of phase composition and surface morphology of compositions that involve both reduction of oxides of molybdenum and its suboxides formation and occurrence of chemical reactions between oxides with formation of zinc molybdate.

## References

- [1] Queeney K., Friend C.: J. Phys. Chem., 2000, **104**, 409. <https://doi.org/10.1021/jp991994m>
- [2] Bacaksiz E., Parlak M., Tomakin M. *et al.*: J. Alloy. Compd., 2008, **466**, 447. <https://doi.org/10.1016/j.jallcom.2007.11.061>
- [3] Wang J., Cao J., Fang B. *et al.*: Mater. Lett., 2005, **59**, 1405. <https://doi.org/10.1016/j.matlet.2004.11.062>
- [4] Rumyantsev R., Il'in A., Pazukhin I.: Theor. Exp. Chem., 2011, **47**, 41. <https://doi.org/10.1007/s11237-011-9182-1>
- [5] Iglesia E., Spivey J., Fleisch T. (Eds.): Studies in Surface Science and Catalysis. Elsevier Science B.V., Amsterdam 2001.
- [6] Beale A., Sankar G.: Chem. Mater., 2013, **15**, 146. <https://doi.org/10.1021/cm020463z>
- [7] Dubovik A., Vostretsov Y., Grinyov B. *et al.*: Acta Phys. Pol. A, 2010, **117**, 15. <https://doi.org/10.12693/APhysPolA.117.15>
- [8] Keereeta Y., Thongtem T., Thongtem S.: Superlattice Microst., 2014, **69**, 253. <https://doi.org/10.1016/j.spmi.2014.02.011>
- [9] Cavalcante L., Sczancoski J., Siu Li M. *et al.*: Colloid Surface A, 2012, **396**, 346. <https://doi.org/10.1016/j.colsurfa.2011.12.021>
- [10] Chambon S., Lionel D., Lahaye M. *et al.*: Materials, 2012, **5**, 2521. <https://doi.org/10.3390/ma5122521>
- [11] Liang Y., Liu H., Yang G.: Cryst. Growth Des., 2012, **12**, 4487. <https://doi.org/10.1021/cg3006629>
- [12] Peng C., Gao L., Yang S., Sun J.: Chem. Commun., 2008, 5601. <https://doi.org/10.1039/b812033a>
- [13] Omran Z., Farid T., El Bellihi A.: Commun. Fac. Sci. Univ. Ank. Series B., 1999, **45**, 9.
- [14] Ryu J., Koo S.-M., Yoon Y.-W.: Mater. Lett., 2006, **60**, 1702. <https://doi.org/10.1016/j.matlet.2005.12.018>
- [15] Zazhigalov V., Sachuk E., Kopachevskaya N. *et al.*: Theor. Exp. Chem., 2016, **52**, 96. <https://doi.org/10.1007/s11237-016-9456-8>
- [16] Boldyrev V.: Thermochim. Acta., 1987, **110**, 303. [https://doi.org/10.1016/0040-6031\(87\)88239-4](https://doi.org/10.1016/0040-6031(87)88239-4)
- [17] Bang J., Suslick K.: Adv. Mater., 2010, **22**, 1039. <https://doi.org/10.1002/adma.200904093>
- [18] Shevchuk L., Starchevskyy V.: Kavitatsiya. Fizychni, Khimichni, Biologichni i Technologichni Aspekty. Lviv 2014.
- [19] Zazhigalov V., Sydorchuk S., Khalameida V., Starchevskyy V.: Sonokhimiya dlya Zahystu Dovkillya: Syntez Katalizatoriv ta Zmenshennya Zabrudnen. Lviv 2016.
- [20] Bhanvase B., Patel M., Sonawane S., Pandit A.: Ultrason. Sonochem., 2016, **18**, 311. <https://doi.org/10.1016/j.ultsonch.2015.08.007>
- [21] Bhanvase B., Kadam V., Rode T. *et al.*: Int. J. Nanosci., 2015, **14**, 1550014. <https://doi.org/10.1142/S0219581X15500143>
- [22] Patel M., Bhanvase B., Sonawane S.: Ultrason. Sonochem., 2013, **20**, 906. <https://doi.org/10.1016/j.ultsonch.2012.11.008>
- [23] Karekar S., Bhanvase B., Sonawane S. *et al.*: Chem. Eng. Proc., 2015, **87**, 51. <https://doi.org/10.1016/j.cep.2014.11.010>
- [24] Smith R. and Rohrer G.: J. Solid State Chem., 1996, **124**, 104. <https://doi.org/10.1006/jssc.1996.0213>
- [25] Dang J., Zhang G.-H., Chou K.-C.: High Temp. Mater. Proc., 2014, **33**, 305. <https://doi.org/10.1515/htmp-2013-0061>
- [26] Klinbumrung A., Thongtem T.: J. Nanomat., 2012, **10**, 1. <https://doi.org/10.1155/2012/930763>
- [27] Collongues R.: La non-stoechiometric. Masson et C<sup>ie</sup>, Editeurs, Paris 1971.
- [28] Chiang T., Yeh H.: Materials, 2013, **6**, 4609. <https://doi.org/10.3390/ma6104609>
- [29] Stoyanova A., Iordanova R., Mancheva M., Dimitriev Y.: J. Optoelectron. Adv. M., 2009, **11**, 1127.
- [30] Dimitriev Y., Iordanova R. *et al.*: Eur. J. Glass Sci. Technol. B., 2012, **53**, 254.
- [31] Farag K., Hanafi Z., Dawy M. *et al.*: Canad. J. Pure Appl. Sci., 2010, **4**, 1303.
- [32] Gruber H., Krautz E. *et al.*: Phys. Stat. Sol. A, 1986, **98**, 297. <https://doi.org/10.1002/pssa.2210980134>

Received: November 11, 2016 / November 18, 2016 /

Accepted: January 30, 2016

## ВПЛИВ УЛЬТРАЗВУКОВОГО ОБРОБЛЕННЯ НА ВЛАСТИВОСТІ ОКСИДНОЇ ZnO-MoO<sub>3</sub> СИСТЕМИ

**Анотація.** Досліджено вплив ультразвукового оброблення (УЗО) оксидної цинк-молібденової системи ZnO-MoO<sub>3</sub> (Zn:Mo=15:85, 25:75, 50:50, 75:25) на її фізико-хімічні властивості. Методами РФА, ІЧ-ФП та ДТА показано, що таке оброблення приводить до утворення субоксидів молібдену (фаз Магнелі складу Mo<sub>4</sub>O<sub>11</sub> і Mo<sub>8</sub>O<sub>23</sub>) та молібдатів цинку: α-ZnMoO<sub>4</sub>, ZnMo<sub>3</sub>O<sub>10</sub>. Встановлено специфічність впливу співвідношення реагентів на формування цих сполук. Показано, в результаті ультразвукового оброблення відбувається зміна поруваної структури композицій – з непоруваної суміші оксидів утворюються композиції з наявністю мікро- та мезопор, що веде до збільшення питомої поверхні зразків та суттєвого зменшення розміру частинок.

**Ключові слова:** оксид цинку, оксид молібдену, сонохімія, субоксид молібдену, молібдат цинку.